

*Chemical structure drives memory effects in the crystallization of
homopolymers*

Leire Sangroniz^{1*}, Ainara Sangroniz¹, Leire Meabe¹, Andere Basterretxea¹,
Haritz Sardon¹, Dario Cavallo^{2*} and Alejandro J. Müller^{1,3*}

¹POLYMAT and Polymer Science and Technology Department, Faculty of
Chemistry, University of the Basque Country UPV/EHU, Paseo Manuel de
Lardizábal, 3, 20018 Donostia-San Sebastián, Spain.

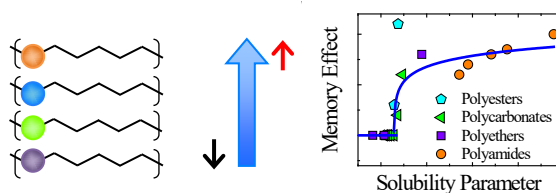
²Department of Chemistry and Industrial Chemistry, University of Genova,
via Dodecaneso, 31 - 16146 Genova, Italy

³IKERBASQUE, Basque Foundation for Science, Bilbao, Spain.

Dedicated to the memory of Dr. Irma Flores

*Corresponding authors: leire.sangroniz@ehu.eus, dario.cavallo@unige.it,
alejandrojesus.muller@ehu.es

For Table of Contents use only:



Abstract

Although the study of melt memory has attracted much interest, the effect of polymer chemical structure on its origin has not been fully elucidated. In this work, we study melt memory effects by Differential Scanning Calorimetry employing a self-nucleation protocol. We use homologous series of homopolymers containing different polar groups and different number of methylene groups in their repeating units: polycarbonate, polyesters, polyethers and polyamides. We show that melt memory in homopolymers is generally controlled by the strength of the intermolecular interactions. The incorporation of methylene groups reduces melt memory effects by decreasing the strength of segmental chain interactions, which is reflected by the decrease in dipolar moments and solubility parameters. This work presents for the first time a unified view of the melt memory effects in different homopolymers.

Keywords: Melt memory; self-nucleation; self-nuclei; polymer crystallization; polymer nucleation.

Introduction

Polymer crystallization depends on thermal history. Temperatures well above the experimental melting temperature are needed to erase memory effects induced by previous crystallization. Once thermal history is erased, an isotropic (or homogeneous) melt is obtained. The crystallization temperature recorded during a cooling scan from the melt in a Differential Scanning Calorimetry (DSC) experiment will be constant, as long as the melting temperature previously applied is high enough. However, when this temperature is not sufficient to produce an isotropic melt, the crystallization process during subsequent cooling accelerates, and higher crystallization temperatures are obtained. This increase in crystallization temperature (and crystallization rate) is known as melt memory effect and it is caused by the self-nuclei produced¹⁻³.

Melt memory effects have been recently reviewed⁴. The exact nature of self-nuclei is still under debate. There are several hypotheses to explain this phenomenon, such as residual orientation of chain segments⁵, small crystal fragments^{2,6}, melt topology effects^{7,8}, or metastable melt states⁸. It has been reported in the literature that melt memory effects depend on: the molecular weight^{3,5,7,10}, the self-nucleation time^{3,5,11}, chain topology^{3,11,12}, and chain confinement¹³⁻¹⁶. In the particular case of copolymers, melt memory depends strongly on the copolymer composition and segregation of non-crystallizable units^{7,17}.

Even though much effort has been made to elucidate the nature of self-nuclei¹⁸⁻²² the study on the persistence of melt memory effects, in terms of the relationship between the width of the self-nucleation *Domain* and the chemical structure of the polymer (i.e., the temperature range where melt memory effects are detected, see below), has not been directly in focus, so far. According to the works

reported in the literature, poly(butylene succinate) (PBS) is one of the homopolymers with the widest melt memory temperature range²³ (about 18 °C), whereas polyolefins such as polyethylene (PE) or polypropylene (PP) show a very narrow melt memory temperature range^{7,20}. Recently, the role of hydrogen bonds in the memory effect of a series of polyamides has been studied by Liu et al.²⁴. The authors have shown that the increase in hydrogen bond density results in a stronger (wider temperature range) melt memory effect. The above results point towards an important role of intermolecular interactions in determining melt memory effect, although a detailed understanding is still missing.

This work aims to determine how polymer chemical structure affects the temperature width of the melt memory effect, by studying homologous series of homopolymers containing different types of polar groups and varying their number of methylene units. We employ polyesters based on diacids and diols, aliphatic polycarbonates²⁵, and polyethers²⁶. Recent literature data on a series of polyamides²⁴ are also included, to extend the study on the role of intermolecular interactions on melt memory to different polymer families, and obtain a more general and unified view.

Experimental Part

Materials

In this work several polymer families have been studied: polycarbonates, polyesters, polyethers and polyamides, see the chemical structure in Figure 1. Except for polyamides which are commercial samples, the other polymers have been synthesized in our laboratory following the procedures described below.

Aliphatic polycarbonates were prepared by polycondensation following a previous report²⁵. Briefly, aliphatic diol, the organocatalyst (4-dimethylaminopyridine, DMAP) and dimethylcarbonate (DMC) were added to a schlenk flask in a 1:0.01:2 molar ratio respectively. The reaction was performed under vacuum. The flask was

first heated to 130°C during 4 hours, and then, it was maintained at 180°C applying a high vacuum and it was left overnight. The polymers obtained were purified dissolving the material in dichloromethane and precipitating in cold methanol. The characterization was consistent with literature data²⁵.

The polyethers were synthesized by bulk polycondensation as reported in the literature²⁶ except polyethylene oxide (PAO2) which is commercial. A mixture of methanesulfonic acid (MSA) and 1,5,7-triazabicyclo[4.4.0.]dec-5-ene (TBD) (3 MSA:1 TBD molar ratio) was employed as catalyst. The Schlenk flask with the corresponding diol and the catalyst was heated up to 130°C during 24 h, then to 180°C during 24 h and finally to 200°C during 24 h under vacuum. The polymer was purified as in the previous case and the characterization was consistent with literature data¹³. The DSC results obtained with commercial polyethylene oxide (PAO2) have been compared with results reported in literature¹³ for a polyethylene oxide with a molecular weight of 1 kg/mol, obtaining the same width of *Domain IIa*.

The polyesters were prepared by melt polycondensation: first esterification was carried out and then the polycondensation under vacuum. The catalyst employed was titanium tetraisopropoxide (TTP) or titanium butoxide (TTB) depending on the polymer. To synthesize the polymer the flask was heated at 190°C during 2 hours, then to 200°C during 2.5 hours, to 230°C during 1 hour under vacuum and finally it was heated to 250°C during 4 hours. In the case of PBA, the reaction was heated at 190°C during 3 hours, then at 210°C during 3 hours and finally at 230°C during 3-4 hours under vacuum as reported in literature. The characterization was consistent with literature data^{23,27}.

The polyamides analysed in this work are commercial and were from Shandong Guangyin New Materials Co., Ltd. Further details can be found in Reference 24.

The melting temperature, melting enthalpy and molecular weight of different materials are shown in Tables S1-S4.

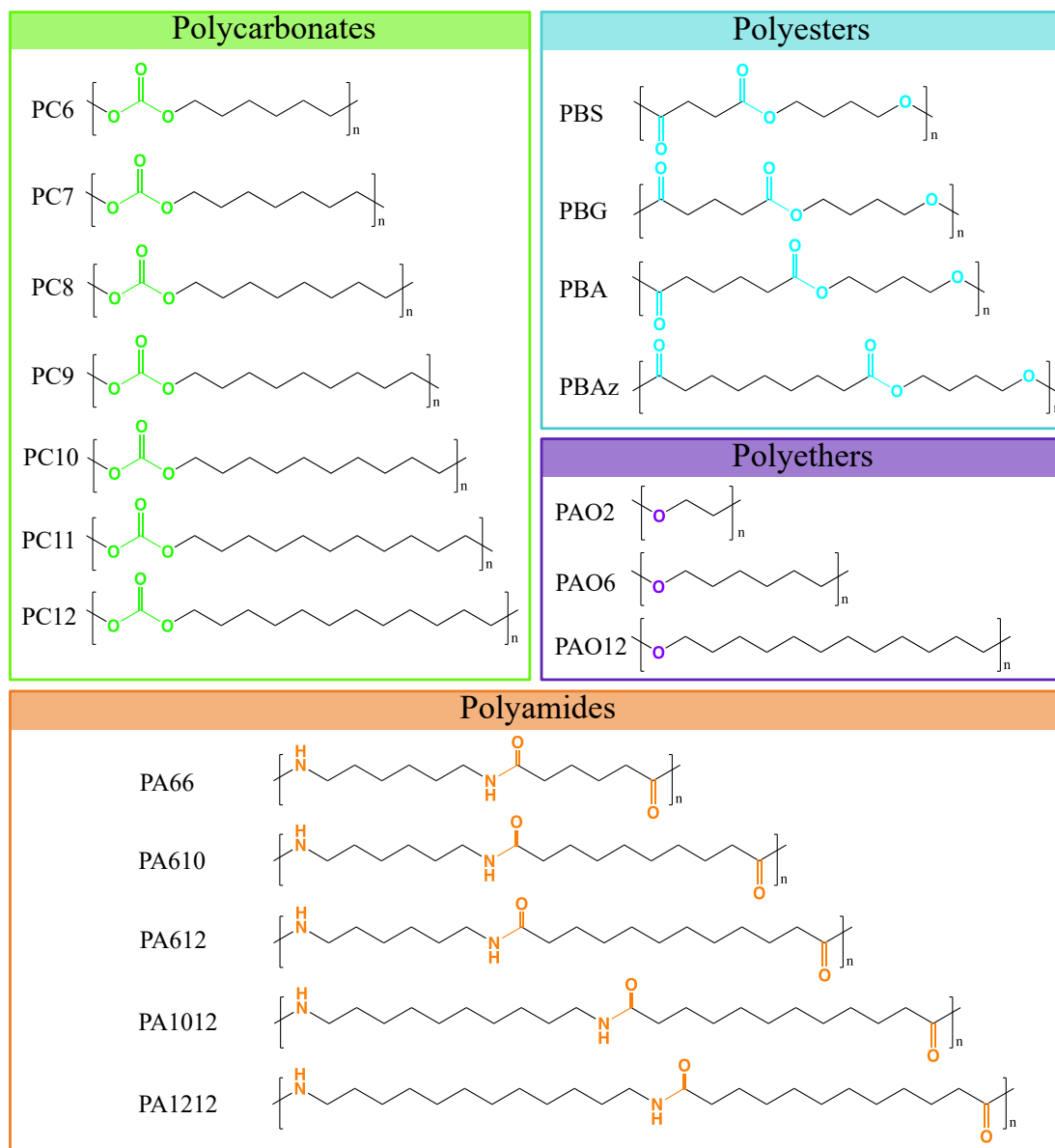


Figure 1. Chemical structure of the repeating unit for the investigated series of homopolymers: polycarbonates, polyesters, polyethers, and polyamides.

Differential Scanning Calorimetric Measurements

To study melt memory effects, a Perkin Elmer 8500 calorimeter has been used which has been calibrated with indium. The measurements were performed with samples of about 3.8-4.2 mg sealed in aluminium pans under nitrogen flow. The self-nucleation procedure was performed following the thermal procedure by Fillon et al.²

(See Figure 2): 1) the sample is heated to temperatures well above the melting temperature (25 or 30°C above the experimental peak melting temperature, to ensure the complete melting of the material) to erase all previous thermal history, and then cooled down at a constant rate to obtain a standard crystalline state, 2) then the polymer is heated to a self-nucleation temperature, T_s , and held there for 5 min, 3) finally, the sample is re-crystallized by cooling and later heated to analyze the newly formed crystals. Depending on the selected T_s temperature, different melt states or *Domains* can be obtained, which can be distinguished by analyzing the cooling from T_s temperature and the subsequent heating scans^{2,3} (See Note 1 in SI).

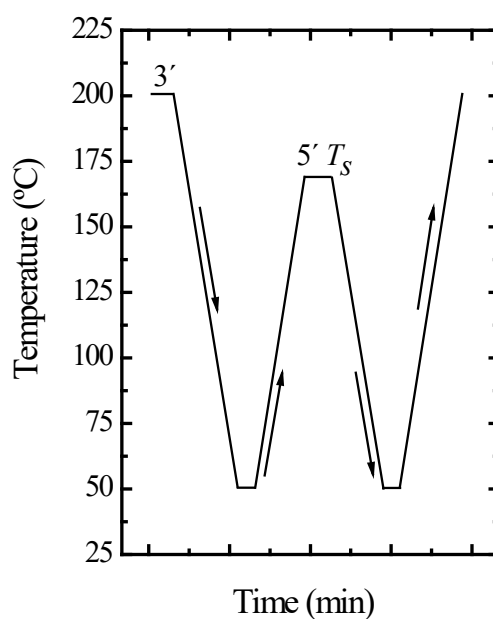


Figure 2. Thermal procedure employed in the self-nucleation procedure.

Results and Discussion

In Figure 3, a representative example of the self-nucleation behavior of the PC6 sample employed here is shown. At self-nucleation temperatures above 68 °C, the crystallization temperature does not change with the selected T_s and is equal to the

standard crystallization temperature, $T_c = 29$ °C. The sample is in *Domain I* or melting *Domain*^{2,3}.

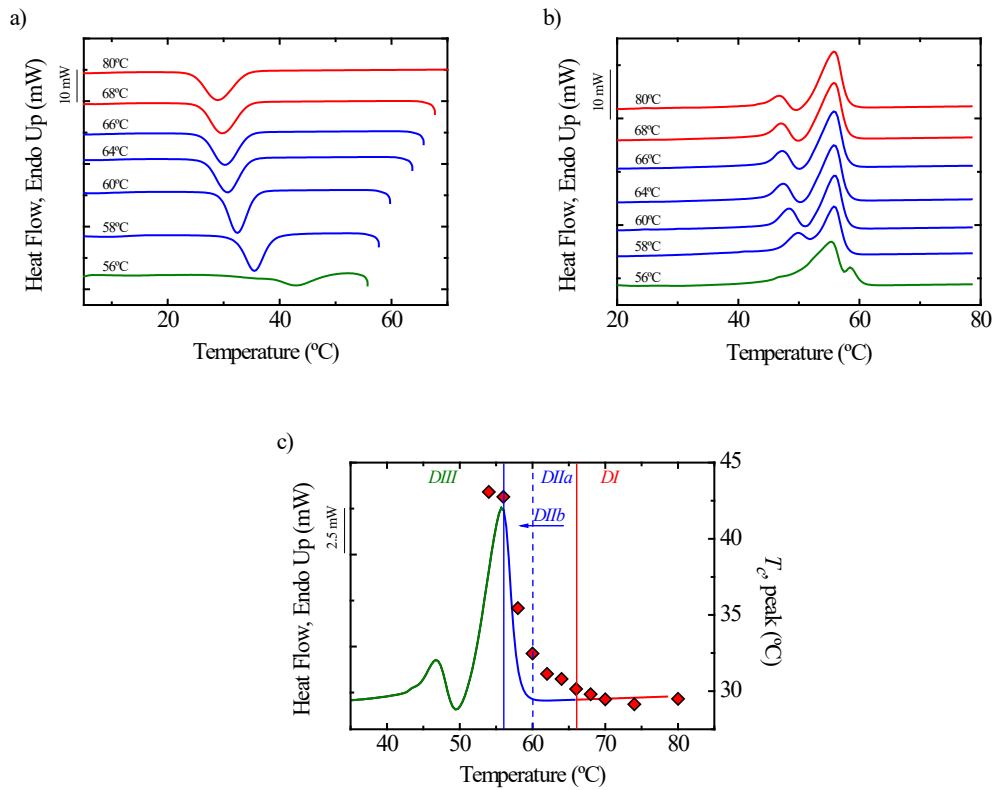


Figure 3. a) Cooling DSC scans of PC6 from the indicated T_s temperatures, b) subsequent heating scans and c) crystallization temperature as a function of T_s superimposed of the melting endotherm. The vertical lines mark the transition temperature between different Domains. Domain II is divided into two sections: DIIa, where the material is in the self-nucleated molten state, and DIIb, where crystalline self-seeds are responsible for the temperature increase.

When the self-nucleation temperature is reduced to values in the range of 66 °C to 58 °C, there is a significant increase in the crystallization temperature in comparison with the standard value, see Figure 3a. This increase results from the presence of self-nuclei that drastically enhances the nucleation density, so in this temperature range, the material is in the *self-nucleation Domain* or *Domain II*. More

specifically, the melting is not complete until 60 °C, since the DSC curve does not reach the baseline until this temperature. For temperatures above 60 °C, the increase of crystallization temperature truly results from the presence of self-nuclei, or melt memory effect, and this temperature range is called *DIIa*²². The region at a lower temperature, where a fraction of unmolten crystals remains and causes self-nucleation, is called *DIIb*²² (and is characteristic of self-seeding⁴). For this PC6 the *DIIa* temperature range is about 6 °C, which is a relatively wide temperature range.

When the self-nucleation temperature is below 56 °C, besides the increase in T_c during the cooling scans, an additional melting peak upon heating is observed in Figure 3b. This peak corresponds to the melting of annealed crystals and marks the transition to *Domain III* in which self-nucleation and annealing occur^{2,3}.

All the melting endotherms show two melting peaks, Figure 3b, independently of the T_s temperature. Multiple melting endotherms can result from the presence of different polymorphisms or from the reorganization of crystals, i.e., partial melting and subsequent crystallization during heating. Considering the studies carried out with PC7 employing WAXS, the presence of different polymorphisms has been ruled out²⁷. If the heating curves corresponding to *Domain I* and *Domain II* are considered, the melting peak at lowest temperature corresponds to less stable crystals and the second one to the more stable recrystallized ones. When T_s temperature decreases from 66 to 58 °C, a shift of the lowest T_m peak towards higher temperature is observed. It should be considered that when cooled from lower T_s temperatures, the polymer re-crystallizes at higher temperatures, hence forming more stable crystals. For T_s temperatures within *Domain I* and *Domain II* the same end-point melting temperature is obtained as in all cases there is a significant population of more stable recrystallized crystals. Finally, if the T_s temperatures corresponding to *Domain III* are

considered, i.e., T_s temperature 56 °C in Figure 3b, two peaks are observed, the one at lower temperature corresponds to the more stable crystals, while the second is due to the annealed residual crystals at T_s , since this small peak is shifted to higher temperatures in comparison with the results obtained for higher T_s .

In Figure 3c, the crystallization temperature of PC6 as a function of T_s temperature in the x-axis has been plotted superposed to the standard melting endotherm. Vertical lines divide the temperature range into three different *Domains*. *Domain II* is further divided into two sections²² as mentioned before: at low temperatures *DIIB*, in which according to the DSC there are still crystal fragments; and *DIIA* where there are no crystal fragments but the crystallization temperature increases due to the presence of self-nuclei.

According to the methodology discussed above concerning PC6, the width of *Domain II*, *Domain IIA*, and *Domain IIB* are determined for a series of polyesters, polycarbonates, and polyethers. Data corresponding to polyamides obtained by Liu et al.²⁴ and to poly(ethylene oxide) are also included in the discussion for comparison purposes. Before discussing the results obtained for the different polymer families it should be taken into account that the time spent at T_s temperature, i.e., t_s , may change the limits between the different *Domains*. However, in previous literature it has been shown for other systems that the effect of time on the measured re-crystallization temperature is generally small or negligible at least for short times^{2,20}. In any case, in this work the same t_s time has been employed for all the polymers.

On the other hand, we note that the molar mass of the various samples is not exactly the same. In a previous study performed by some of us, it was shown for PCL that, despite varying the molar mass about one order of magnitude (from 26 kg to 195 kg/mol), the width of the melt memory effect was practically unaffected²¹. In the case

of the polymer families considered in this work the differences in the molecular weight are below one order of magnitude, being at most a factor 6 for the polyesters. The only exception is PEO, see Experimental Part. Therefore, according to previous literature results, the molar mass of the sample would not affect the results of the present work.

Figure 4 shows the width of *Domain II* and *Domain IIa* for the different polymer families as a function of the number of methylene groups in their repeating unit. The width of *Domain IIb* as a function of the number of methylene groups is shown in the Supporting Information, Figure S1. There is a clear reduction of *Domain II* width for all the considered polymer series (Figure 4a) as the number of methylene groups increases. This pronounced decrease is mostly due to the reduction in *IIa* width (Figure 4b). We will consider the results of *Domain IIa* and *Domain IIb* separately.

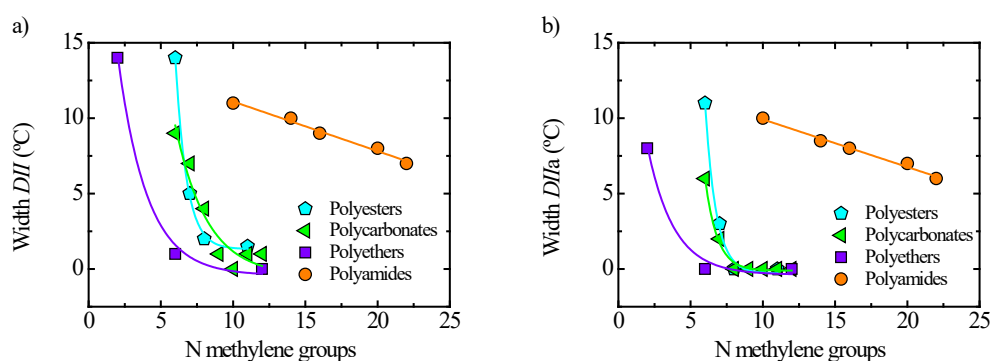


Figure 4. The width of a) *Domain II* and b) *Domain IIa* for polyesters, polycarbonates, polyethers and polyamides as a function of the number of methylene groups. The lines have been drawn to guide the eye.

In the case of *Domain IIa* (Figure 4b), polyesters and polycarbonates with 6 methylene units show a width of 11 and 6 °C, respectively. However, with the

incorporation of more methylene units, the *DIIa* width reduces drastically, down to its disappearance in polymers containing the two polar groups and 8 methylene units. Regarding polyethers, PEO, which only contains 2 methylene groups, displays a *Domain IIa* of 8 °C, while polyethers with 6 methylene groups or more do not show any melt memory effect.

Polyamides, on the other hand, show different behavior in Figure 4b. The incorporation of methylene units reduces the width of *Domain II*, but even with 22 methylene groups, the sample still shows a *Domain IIa* of 7 °C²⁴. Contrary to the rest of the polymer series studied in this work, for polyamides, *Domain IIa* does not vanish in the explored range of methylene units. These results are probably due to the higher strength of hydrogen bonds in polyamides, as it will be discussed in more detail below.

Domain IIb also reduces its width as the number of methylene groups in the repeating units decreases (see Figure S1 in SI), even though the data is more scattered. In comparison with *DIIa*, the width of *Domain IIb* is smaller and relatively constant with the number of methylene units.

As reported before, the molecular weight of the samples can affect the width of *Domains*^{5,7,10}. However, in this study, the variations in the molecular weight for the same polymer family are not meaningful (see Table S1-S4 in SI). In addition, no correlation between the width of *Domain II* and the crystallinity degree can be derived, see SI Table S1-S4. Remarkably, the trends displayed by melt memory effect with methylene units number are found in different polymer classes, despite the differences in crystalline structures between them. It has been previously reported for polycarbonates that a subtle odd-even effect in the melting temperature²⁵ exists when the number of methylenic units is varied along the repeating unit. However, according

to the present results it seems that such minor even-odd effect does not affect the width of *Domain II*.

The results presented above demonstrate the key role of intramolecular interactions between chain segments on melt memory, as they determine the width of *Domain II*. In fact, if we consider the different polymer families, polyamides have the largest interactions due to the presence of strong hydrogen bonding groups. Polyesters can only form weak hydrogen bonds due to the electronegativity of the ester group atoms, as it has been reported for PBS²⁸ and PCL²⁹. Finally, polyethers and polycarbonates can only form weak dipole-dipole interactions.

To gain more insights, the transition temperatures between *Domain II* and *Domain I* are shown as a function of the endpoint of the DSC melting endotherm for the different polymer series in Figure 5.

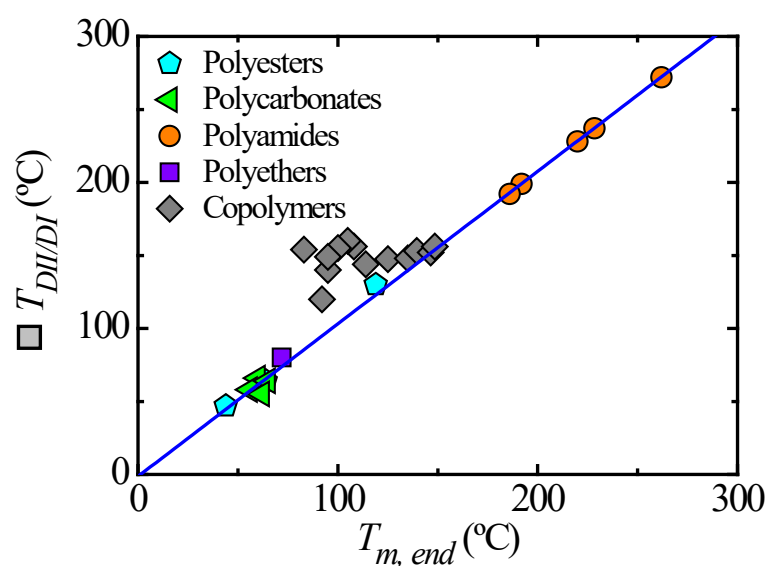


Figure 5. Transition temperature between *Domain II* and *Domain I* as a function of the end-point of the melting endotherm for the different series of polymers considered.

Data reported in literature for random copolymers based on PP and PE have been included^{7,17,20}. The line corresponds to a linear fit of the homopolymers' data.

The data from the different polymers follow the same linear trend in Figure 5, reflecting a direct relationship between the stability of the self-nuclei ($T_{DII/DI}$), with the ultimate stability of the original crystals. Considering that the melting temperature depends mainly on the intermolecular forces between chains³⁰⁻³², being the melting entropy largely invariant among various polymer types, the direct relationship between $T_{DII/DI}$ and $T_{m,end}$ corroborates the deductions drawn from Figure 4. Figure 5 suggests that in homopolymers of various chemical nature, despite the specific type of interactions, the same forces that govern the melting of the polymer crystals are also involved in the persistence of the self-nucleation effect above the experimental melting temperature. However, the same relationship does not hold in random copolymers, since the corresponding data show large deviations from the common line of the homopolymers. It can be deduced that fundamentally different mechanisms drive the memory effect in the two polymer classes. While for the presently investigated homopolymers containing different polar groups intermolecular forces seems to play a dominant role both in dictating crystals' melting point and self-nuclei thermal stability. for random copolymers, melt memory is caused by the complex topological constraints created in the amorphous phase by the process of crystallizable sequence selection during crystallization, as suggested in the literature⁷.

To attempt a comprehensive discussion of memory effects in different polymer families, under the hypothesis of a major role of interactions between chain segments, the strength of such interactions is quantified for the considered samples in the next section.

One way to estimate the extent of intermolecular interactions (including dispersion forces, polar forces and hydrogen bonds) is the solubility parameter, which can be calculated from the cohesive energy as well as from molar attraction constant^{30,33} (see Note 2 in SI). Given that the polymers studied have polar groups, in addition to dispersion forces, dipole-dipole interactions should be present. Thus, they can be taken into account by calculating the dipolar moment, which directly determines the interaction forces between permanent dipoles.

Figure 6a shows the extent of melt memory, expressed as the width of *Domain IIa*, as a function of semi-empirically calculated values (employing group contribution theory³⁰) of the solubility parameter for all the homologous polymer series. Although the data is somewhat scattered, above a certain minimum value, there is a clear increasing trend of the memory effect as the solubility parameter (and hence intermolecular forces) increases.

A normalized version of Figure 6a can be found in Figure 6b, where the solubility parameter was divided by the molecular weight of the repeating unit of each polymer considered. Methylene units only contribute with dispersion forces to the intermolecular interactions and “dilute” the dipolar interaction strength. The normalized data for each series presents a smooth trend, as the effect of the different number of methylene units is taken into account. Figure 6b shows for each polymer family a different trend (in comparison to the rough approximation of a common trend in Figure 6a): polyesters, polyethers and polycarbonates show a sudden increase at a certain normalized solubility value, whereas polyamides show a more progressive increase.

In Figure 6c the width of *Domain IIa*, or the extent of the melt memory effect, is plotted against the molecular dipolar moment, which has also been calculated

employing group contribution theory³⁰, normalized by the molecular weight of the repeating unit.

It can be seen in Figure 6c that polyesters, polycarbonates and polyethers display analogous trends. Figure 6b and 6c show that the memory effect is absent until a critical value of normalized solubility parameter and dipolar moment, in the range 0.08-0.13 J^{1/2}/cm^{3/2}g and 3-4 x 10⁻³ D/g, above which the width of *Domain IIa* becomes larger than zero and increases proportionally to the considered parameter. Interestingly, the critical values of normalized solubility parameter or dipolar moment are dependent on the type of polar groups in the polymer, increasing in the order polyesters, polycarbonate and polyethers. It seems that this critical value is larger for weaker dipoles, and this explains why polyethers with 6 methylene groups do not show any *Domain IIa*.

Polyamides show a somewhat different behavior, as in this case the critical solubility parameter or dipolar moment needed to show melt memory effects (i.e., a finite value of *Domain IIa*) is really small; i.e., roughly below 0.0189 J^{1/2}/cm^{3/2}g or 0.0017 D/g respectively. As such, polyamides display *Domain IIa*, even when there are 22 methylene groups per repeating unit, and therefore the polymer has low dipolar moment and low solubility parameter. This is probably due to the strong interactions of hydrogen bonds²⁴, which might not be properly accounted for by the solubility parameter or dipolar moment. Although polyamides have a wider *Domain IIa* in comparison with the other polymer series, a saturation value seems to be reached.

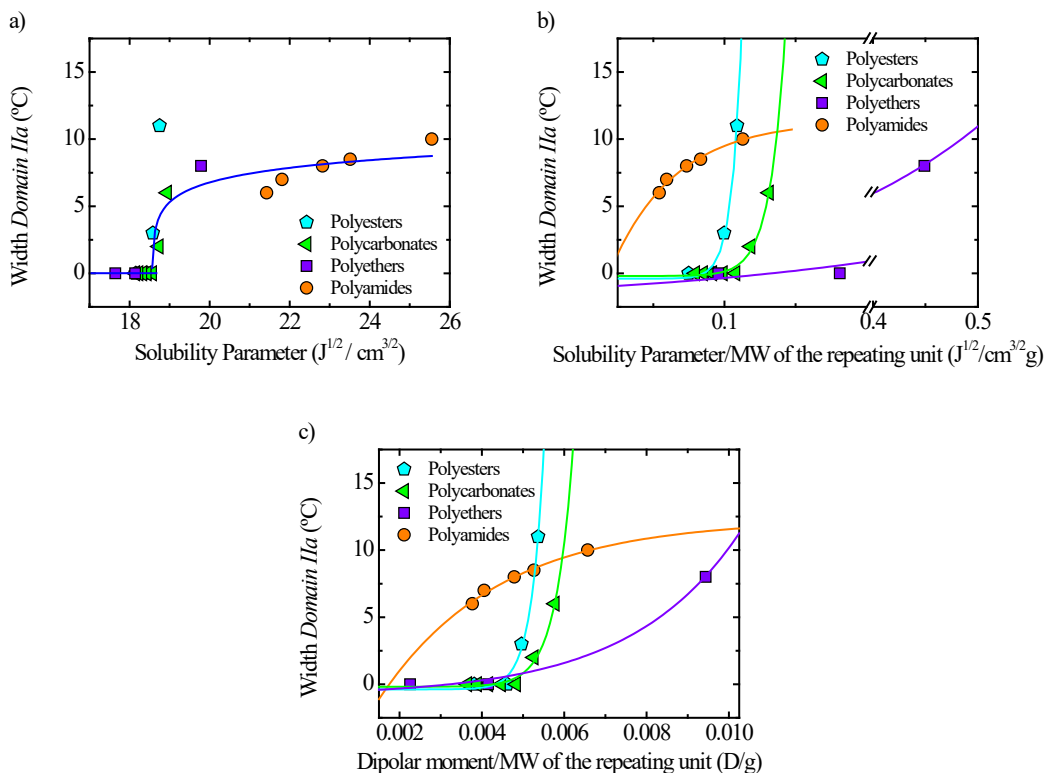


Figure 6. The width of Domain II for polyesters, polycarbonates, polyethers and polyamides as a function of a) the solubility parameter, b) the solubility parameter divided by the molecular weight of the repeating unit and c) the dipolar moment divided by the molecular weight of the repeating unit.

Therefore, we have demonstrated that the stability of self-nuclei in the melt clearly depends on the strength of intermolecular interactions. If the material has strong interactions, i.e., high dipolar moment or solubility parameter, the forces associated to the self-nuclei require a high thermal energy to be broken. In other words, polymers with stronger intermolecular interactions generally display wider melt memory effects.

Conclusions

In this work it has been shown that the incorporation of methylene groups in the repeating units of polyesters, polycarbonates, polyethers and polyamides reduces the width of *Domain IIa*. The reduction of *Domain IIa* results from the decrease of the strength of the interactions, which is reflected by the decrease of dipolar moment or by the decrease of the solubility parameter. For the different polymers examined here, there is a critical dipolar moment or solubility parameter value that the polymer should surpass in order to display melt memory effects or *Domain IIa*. Overall, in this work we have demonstrated that the melt memory effect for homologous series of different polymer families is governed by the intermolecular interactions of the chains, thereby proposing a unified view of the melt memory effects in homopolymers.

Associated Content

Supporting Information

Table S1-S4: Melting temperature, melting enthalpy and molecular weight of the different polymers studied; Figure S1: width of *Domain IIb* as a function of number of methylene groups.

Author Information

Corresponding Authors

*Emails: leire.sangroniz@ehu.eus, dario.cavallo@unige.it,
alejandrojesus.muller@ehu.es

ORCID

Leire Sangroniz: 0000-0003-0714-3154

Ainara Sangroniz: 0000-0003-3508-9220

Leire Meabe: 0000-0003-1449-1544

Andere Basterretxea: 0000-0003-0337-3593

Haritz Sardon: 0000-0002-6268-0916

Dario Cavallo: 0000-0002-3274-7067

Alejandro J. Müller: 0000-0001-7009-7715

Note: The authors declare no competing financial interest

Acknowledgments

We acknowledge funding from MINECO MAT2017-83014-C2-1-P project, and from the Basque Government through grant IT1309-19. L. S acknowledges FPU predoctoral grant and the postdoctoral grant from Basque Government. We would also like to thank the financial support provided by the BIODEST project; this project has received funding from the European Union's Horizon 2020 research and innovation programme under the Marie Skłodowska-Curie grant agreement No 778092.

References

(1) Blundell, D. J.; Keller, A.; Kovacs, A. J. A new self-nucleation phenomenon and its application to the growing of polymer crystals from solution. *J. Polym. Sci. B Polym. Lett.* **1966**, *4*, 481-486.

(2) Fillon, B.; Wittmann, J. C.; Lotz, B.; Thierry, A. Self-nucleation and recrystallization of isotactic polypropylene (α phase) investigated by differential scanning calorimetry. *J. Polym. Sci. B Polym. Phys.* **1993**, *31*, 1383-1393.

- (3) Michell, R. M.; Mugica, A.; Zubitur, M.; Müller, A. J. Self-nucleation of crystalline phases within homopolymers, polymer blends, copolymers, and nanocomposites. *Adv. Polym. Sci.* **2017**, *276*, 215–256.
- (4) Sangroniz, L.; Cavallo, D.; Müller, A. J. Memory effects on polymer crystallization. Submitted to *Macromolecules*, 2020.
- (5) Lorenzo, A. T.; Arnal, M. L.; Sánchez, J. J.; Müller, A. J. Effect of annealing time on the self-nucleation behavior of semicrystalline polymers. *J. Polym. Sci. B Polym. Phys.* **2006**, *44*, 1738–1750.
- (6) Xu, J.; Ma, Y.; Hu, W.; Rehahn, M.; Reiter, G. Cloning polymer single crystals through self-seeding. *Nat. Mater.* **2009**, *8*, 348-353.
- (7) Reid, B. O.; Vadlamudi, M.; Mamun, A.; Janani, H.; Gao, H.; Hu, W.; Alamo, R. G. Strong memory effect of crystallization above the equilibrium melting point of random copolymers. *Macromolecules* **2013**, *46*, 6485–6497.
- (8) Luo, C.; Sommer, J.-U. Frozen topology: Entanglements control nucleation and crystallization in polymers. *Phys. Rev. Lett.* **2014**, *112*, 195702.
- (9) Muthukumar, M. Communication: Theory of melt-memory in polymer crystallization. *J. Chem. Phys.* **2016**, *145*, 031105.
- (10) Pérez, R. A.; Córdova, M. E.; López, J. V.; Hoskins, J. N.; Zhang, B.; Grayson, S. M.; Müller, A. J. Nucleation, crystallization, self-nucleation and thermal fractionation of cyclic and linear poly(ϵ -caprolactone)s. *React. Funct. Polym.* **2014**, *80*, 71–82.
- (11) Chen, X.; Qu, C.; Alamo, R. G. Effect of annealing time and molecular weight on melt memory of random ethylene 1-butene copolymers. *Polym. Int.* **2019**, *68*, 248-256.

- (12) Zaldua, N.; Liénard, R.; Josse, T.; Zubitur, M.; Mugica, A.; Iturrospe, A.; Arbe, A.; De Winter, J.; Coulembier, O.; Müller, A. J. Influence of chain topology (cyclic versus linear) on the nucleation and isothermal crystallization of poly(L-lactide) and poly(D-lactide). *Macromolecules* **2018**, *51*, 1718-1732.
- (13) Arnal, M. L.; López-Carrasquero, F.; Laredo, E.; Müller, A. J. Coincident or sequential crystallization of PCL and PEO blocks within polystyrene-*b*-poly(ethylene oxide)-*b*-poly(ϵ -caprolactone) linear triblock copolymers. *Eur. Polym. J.* **2004**, *40*, 1461-1476.
- (14) Wen, X.; Su, Y.; Shui, Y.; Zhao, W.; Müller, A. J.; Wang, D. Correlation between grafting density and confined crystallization behavior of poly(ethylene glycol) grafted to silica. *Macromolecules* **2019**, *52*, 1505-1516.
- (15) Michell, R. M.; Müller, A. J. Confined crystallization of polymeric materials. *Prog. Polym. Sci.* **2016**, *54-55*, 183-213.
- (16) Michell, R. M.; Blaszczyk-Lezak, I.; Mijangos, C.; Müller, A. J. Confinement effects on polymer crystallization: From droplets to alumina nanopores. *Polymer* **2013**, *54*, 4059-4077.
- (17) Marxsen, S. F.; Alamo, R. G. Melt-memory of polyethylenes with halogen substitution: Random vs. precise placement. *Polymer* **2019**, *168*, 168-177.
- (18) Li, W.; Wu, X.; Chen, X.; Fan, Z. The origin of memory effect in stereocomplex poly (lactic acid) crystallization from melt state. *Eur. Polym. J.* **2017**, *89*, 241-248.
- (19) Zhang, H.; Shao, C.; Kong, W.; Wang, Y.; Cao, W.; Liu, C.; Shen, C. Memory effect on the crystallization behavior of poly(lactic acid) probed by infrared spectroscopy. *Eur. Polym. J.* **2017**, *91*, 376–385.

(20) Sangroniz, L.; Cavallo, D.; Santamaria, A.; Müller, A. J.; Alamo, R. G. Thermorheologically complex self-seeded melts of propylene-ethylene copolymers. *Macromolecules* **2017**, *50*, 642-651.

(21) Sangroniz, L.; Barbieri, F.; Cavallo, D.; Santamaria, A.; Alamo, R. G.; Müller, A. J. Rheology of self-nucleated poly(ϵ -caprolactone) melts. *Eur. Polym. J.* **2018**, *99*, 495–503.

(22) Sangroniz, L.; Alamo, R. G.; Cavallo, D.; Santamaria, A.; Müller, A. J.; Alegría, A. Differences between isotropic and self-nucleated PCL melts detected by dielectric experiments. *Macromolecules* **2018**, *51*, 3663–3671.

(23) Arandia, I.; Mugica, A.; Zubitur, M.; Arbe, A.; Liu, G.; Wang, D.; Mincheva, R.; Dubois, P.; Müller, A. J. How composition determines the properties of isodimorphic poly(butylene succinate-ran-butylene azelate) random biobased copolymers: From single to double crystalline random copolymers. *Macromolecules* **2015**, *48*, 43–57.

(24) Liu, X.; Wang, Y.; Wang, Z.; Cavallo, D.; Müller, A. J.; Zhu, P.; Zhao, Y.; Dong, X.; Wang, D. The origin of memory effects in the crystallization of polyamides: Role of hydrogen bonding. *Polymer* **2020**, 122117, in press.

(25) Meabe, L.; Lago, N.; Rubatat, L.; Li, C.; Müller, A. J.; Sardon, H.; Armand, M.; Mecerreyes, D. Polycondensation as a versatile synthetic route to aliphatic polycarbonates for solid polymer electrolytes. *Electrochimica Acta* **2017**, *237*, 259-266.

(26) Basterretxea, A.; Gabirondo, E.; Jehanno, C.; Zhu, H.; Flores, I.; Müller, A. J.; Etxeberria, A.; Mecerreyes, D.; Coulembier, O.; Sardon, H. Polyether synthesis by bulk self-condensation of diols catalyzed by non-eutectic acid-base organocatalysts. *ACS Sustainable Chem. Eng.* **2019**, *7*, 4103-4111.

(27) Arandia, I.; Meabe, L.; Aranburu, N.; Sardon, N.; Mecerreyes, D.; Müller, A. J. Influence of chemical structures on isodimorphic behavior of three different copolycarbonate random copolymer series. *Macromolecules* **2020**, *53*, 669-681.

(28) Tatsuoka, S.; Sato, H. Stress-induced crystal transition of poly(butylene succinate) studied by terahertz and low-frequency Raman spectroscopy and quantum chemical calculation. *Spectrochim. Acta A* **2018**, *197*, 95-102.

(29) Funaki, C.; Yamamoto, S.; Hoshina, H.; Ozaki, Y.; Sato, H. Three different kinds of weak C-H \cdots C=O inter- and intramolecular interactions in poly(ϵ -caprolactone) studied by using terahertz spectroscopy, infrared spectroscopy and quantum chemical calculations. *Polymer* **2018**, *137*, 245–254.

(30) Van Krevelen, D. W. *Properties of Polymers*; Elsevier: Amsterdam, 1972.

(31) Askadskii, A. A., Matveev, Y. I.; Slonimskii, G. L., Korschik, V. V., Dokl.Akad. Nauk. Effect of inter-molecular interaction energy of different types of bonds on temperature of polymer melting. *SSSR* **1978**, *238*, 592.

(32) Bunn, C. W. The melting points of chain polymers. *J. Polym. Sci. B Polym. Phys.* **1996**, *34*, 799-819.

(33) Darby, J. R.; Touchette, N. W.; Kern, S. Dielectric constants of plasticizers as predictors of compatibility with polyvinyl chloride. *Pol. Eng. Sci.* **1967**, *7*, 295-309.